Boundary-Layer Meteorol (2010) 137:441–457
DOI 10.1007/s10546-010-9536-6

ARTICLE

Coupling Mesoscale Modelling with a Simple Urban Model: The Lisbon Case Study

Efisio Solazzo · Silvana Di Sabatino · Noel Aquilina · Agnes Dudek · Rex Britter

Received: 12 May 2008 / Accepted: 3 August 2010 / Published online: 29 August 2010

Abstract The ongoing trend of urbanisation worldwide is leading to a growing requirement for detailed flow and transport parameterisations to be included within numerical weather prediction (NWP) models. Such models often employ a simple roughness parameterisation for urban areas, which is not particularly accurate in predicting or assessing the flow and dispersion at street scale. Moreover, this kind of parameterisation offers too poor a representation of the mechanical and thermal forcing exerted by urban areas on the larger scale flow. At present, high computational costs and long simulation running times are among the constraints for the implementation of more detailed urban sub-models within NWP models. To overcome such limitations, a downscaling procedure from the atmospheric flow at the synoptic scale to the neighbourhood scale and below, is presented in this study. This is achieved by means of a simple urban model based on a parameterised formulation of the drag exerted by the building on the airflow. Application of the urban model for estimating spatially-averaged mean wind speed and the urban heat island over a selected neighbourhood area in Lisbon, Portugal, is presented. The results show the capability of the urban model to provide more accurate mean wind and temperature profiles. Moreover, the urban model has the advantage of being cost effective, as it requires small computational resources, and thus

E. Solazzo
Division of Environmental Health and Risk Management, School of Geography, Earth and Environmental Sciences, University of Birmingham, Birmingham, UK

S. Di Sabatino
Division of Climatology and Meteorology, Material Sciences Department, University of Salento, Lecce, Italy

N. Aquilina (✉)
Department of Physics, University of Malta, Msida, MSD 2080, Malta
e-mail: noel.aquilina@um.edu.mt

A. Dudek
Norwegian Institute for Air Research, Kjeller, Norway

R. Britter
Massachusetts Institute of Technology, Cambridge, MA, USA

is suitable to be adopted in an operational context. The model is simple enough to be also used to assess how the resolving of urban surface processes may affect those at the larger scales.

Keywords Neighbourhood scale · Spatially-averaged profiles · Urban canopy · Urban heat island

1 Introduction

The European research training network ATREUS (Advanced Tools for Rational Energy Use towards Sustainability, with emphasis on micro-climatic issues in urban application) aimed to optimize the energy efficiency of buildings in relation to their heating, ventilation, and air-conditioning requirements, by means of building simulation models (Papadopoulos and Moussiopoulos 2004). The energy budget of buildings was studied by considering meteorological and micro-climatic conditions through the combination of climate models from mesoscale to the street scale. On the large scale, the numerical mesoscale model MM5 (version 3.6.1) (e.g. Dudhia and Bresch 2002) was used to provide the meteorological field variables used as input for the building simulation models, for a selected neighbourhood area in the city of Lisbon, Portugal. However, study of the energy efficiency of buildings requires detailed information on wind speed and temperature in the urban area, which cannot be provided by mesoscale models. For this reason, both computational fluid dynamics (CFD) and statistical models were used to produce urbanised micrometeorological profiles of wind and temperature, to be also used as input for the building simulation models. The final outputs of the ATREUS network, i.e. applications of the urbanised profiles for the studying of energy efficiency of buildings, are discussed in Oxizidis et al. (2007).

In the present study, an intermediate task of the ATREUS methodology is presented. This consists of downscaling the results from MM5 at the synoptic scale to the smaller street scale, achieved by means of a simple urban model. Results from MM5 were used to provide boundary conditions for the urban model well above the urban area.

Previous studies (e.g., Martilli et al. 2002; Dupont et al. 2004; Lee and Park 2008), proposed detailed methodologies for the so-called "urbanisation" of mesoscale models such as MM5, based on a comprehensive set of equations linking the synoptic to the street scale circulation, and including parameterisations for the turbulent exchange processes of momentum and mass. However, while on the one hand such methodologies allow to produce very detailed results, on the other hand they usually require a large amount of input data, which limits their use in fast-response operational models (Best 2005; Oxizidis et al. 2007). A crucial question to be addressed is to what level of detail should mesoscale models include the heterogeneities of urban areas. This question is directly linked to the size of the grid cells used to solve the equations in the model. Too coarse a resolution would result in a poor characterisation of the urban effects on the large flow and surface energy balance. By contrast, studies of the flow around individual buildings, or small portions of urban areas, using for example CFD models, are computationally demanding and require many input details that are site-specific (Best 2005). Such level of accuracy does not significantly improve the general understanding of flow and temperature distributions at the urban scale and below, and cannot be obtained using available numerical weather prediction (NWP) models.

The current challenge is to develop a cost-effective methodology to include an urban model capable of dealing with the micro-climate developing within urban areas, and to link it to the larger scales of atmospheric circulation. Such urban model should be detailed enough

to capture salient modifications to the local fields due to the urban area as a whole, but should not require additional computational resources.

Our study proposes a cost effective downscaling procedure for modelling (a) the spatially-averaged mean flow, and (b) the urban heat island (UHI) intensity at the neighbourhood scale for an urban area, using boundary conditions obtained by mesoscale modelling calculations. Several velocity scales are determined and quantified (the friction velocity $u_\star$, the exchange velocity u_E, the in-canopy velocity U_C), and a new methodology for estimating the exchange of mass between the urban canopy layer and the inertial sublayer above based on u_E is proposed. The results achieved are of direct relevance for application to urban flow modelling, building simulation models, NWP, and other environmental applications, such as air quality assessment.

2 Horizontal and Vertical Scales

The atmospheric boundary layer developing over an urban area is usually divided into three major layers: the urban canopy layer (UCL), the roughness sublayer, and the inertial sublayer (Britter and Hanna 2003). The urban canopy layer has a depth equal to that of the buildings; here the flow is directly affected by the local obstacles. The roughness sublayer is assumed to have a depth of 3–5 times the averaged building height H (Cheng and Castro 2002; Kastner-Klein and Rotach 2004). The roughness sublayer is, when horizontally averaged, adapted to the presence of the building canopy (if canopy properties reasonably homogeneous), but it is continually adjusting to the specific buildings it encounters. The inertial sublayer is where the atmospheric boundary layer has adapted to the effect of the underlying urban surface. The inertial sublayer is thus high enough to only "see" the average effect of the buildings and so is adapted to the presence of the canopy, but is not adapted to individual buildings. Above the inertial sublayer, at larger scales, the geostrophic condition is retained, resulting in the balance between the Coriolis and the horizontal pressure gradient forces. In Fig. 1 the aforementioned layers are shown for a cross-section of an idealised urban neighbourhood.

Based on the Monin–Obukhov similarity theory, the wind-speed profile above a rough surface is typically expressed by the logarithmic law, which, under neutral atmospheric conditions, can be expressed as:

$$u(z) = \left(\frac{u_\star}{\kappa}\right) \ln\left(\frac{z-d}{z_0}\right) \tag{1}$$

where $\kappa = 0.40$ is the von Karman constant, $u_\star$ is the friction velocity, z_0 and d are the aerodynamic roughness length and the zero-plane displacement height, respectively. The advantage of using Eq. 1 within NWP models resides in the continuity with the surrounding rural areas, where the same profile as Eq. 1, but with different z_0 and d parameters, is adopted. Moreover, it has a negligible impact on the computational costs (Martilli 2007). On the other hand, disadvantages related to the use of Eq. 1 are of major concern, since it results in $u(z_t) = 0$ for $z_t = d + z_0$. Thus, at $z = z_t$ mesoscale models based on parameterisations similar to Eq. 1 see a flat, rough surface, drastically simplifying the features of the flow below. It is important to notice that d and z_0 have meaning only if Eq. 1 is applied over a statistically homogeneous fetch (Hamlyn et al. 2007). For application over urban areas, d and z_0 need to be defined based on the characteristics of the underlying roughness (Kastner-Klein and Rotach 2004). In Fig. 1 the dashed profile represents a typical output from a mesoscale model that relies on a simple roughness approach. The dotted profile represents a spatially-averaged mean wind-speed profile from within the inertial sublayer (see, for

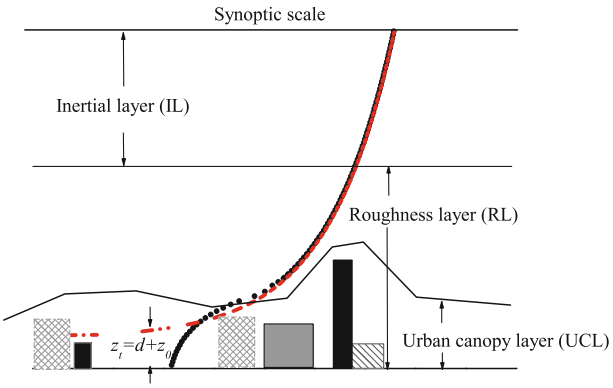

Fig. 1 Logarithmic velocity profile (Eq. 1) (*dashes*) and the spatially-averaged mean wind speed profile (*dots*) in the vicinity of an urban area (adapted from Britter and Hanna 2003)

example, Macdonald 2000; Coceal and Belcher 2004; Di Sabatino et al. 2008). The effect of the urban roughness on the flow field is averaged over an appropriately defined horizontal area, removing the spatial variability associated with individual buildings. One of the desired outcomes of our study is to obtain such a profile. To this scope the area over which the spatial average is computed needs to be defined.

Britter and Hanna (2003) argued that the processes driving the mixing and transport within and above urban areas vary over a large range of spatial scales. Different applications require details at a different level, depending on the spatial scale being analysed. Four horizontal spatial scales were introduced and the corresponding vertical depth identified, each characterised by a different dispersion and fluid dynamics mechanisms:

- Regional scale, the larger surrounding area that is mutually influenced by the city area, extending up to several hundreds km in the horizontal, and throughout the whole depth of the troposphere.
- City scale, over which the urban area varies, i.e. up to 50 km. Its influence is extended over the whole depth of the boundary layer, i.e. up to about 1 km.
- Neighbourhood scale, which bridges the range of scales between street and city scales, i.e. from 0.2 to 10 km in the horizontal, and from the ground up to the lowest 100 m of the atmospheric boundary layer.
- Street scale, up to 200 m in the horizontal, and from the ground up to about 2–3 times the building height vertically.

Our study focuses on the neighbourhood and street scales, at which the meteorological fields are strongly influenced by the building morphology. Therefore, detailed treatment of the canopy structures in mesoscale models is required, as well as additional morphological databases as input (Dupont et al. 2004).

3 Methodology

A simple urban model is introduced with the aim of coupling the larger scale mesoscale circulations with the neighbourhood and street scales, and hence to produce urbanised meteorological vertical profiles. The proposed urban model is based on the spatially-averaged exchange of momentum and mass between the urban canopy layer and the atmosphere above.

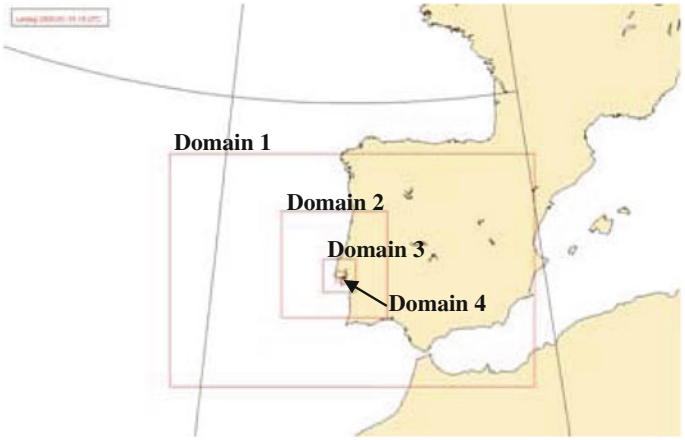

Fig. 2 Lisbon nesting configuration adopted for MM5 simulations

Spatial averaging has the advantage of removing the variability of the flow due to individual obstacles (Kastner-Klein and Rotach 2004; Coceal and Belcher 2004). Thus, buildings are not explicitly resolved within the model, but are parameterised as sources of drag on the airflow (Di Sabatino et al. 2008). The advantage of the proposed urban model is that it is simple to run, needs modest computational resources, and requires a limited number of input data.

In Sect. 3.1, the geometric features of the investigated urban neighbourhood are described, and applications of MM5 simulations to this site are outlined. In Sect. 3.2 the urban model is presented, and in Sect. 4 the results for the spatially-averaged wind speed and temperature profiles are then presented and discussed. In order to apply the urban model, two velocity scales are calculated: $u_\star$ (discussed in Sect. 4.1), and the in-canopy velocity U_C (Sect. 4.2). This latter scale is of direct relevance to urban dispersion modelling, and it is calculated by comparing several parameterisations proposed in the literature. Main conclusions and future work are discussed in Sect. 5.

3.1 MM5 Modelling of the Baixa Area (Lisbon)

The MM5 is a limited-area, terrain-following, high resolution, non-hydrostatic NWP, with sigma-coordinates developed by Penn State University and the National Center for Atmospheric Research. MM5 is designed to simulate or predict mesoscale and regional-scale atmospheric circulations. The model is supported by several auxiliary programs, which are referred to as MM5 (http://www.mmm.ucar.edu/mm5/). In MM5, the boundary conditions are specified in terms of horizontal winds, temperature, pressure, and moisture fields. For the purposes of our study, boundary conditions were obtained from the ERA-40 archive (http://data.ecmwf.int/data), which contains data with a timestep of six hours and a $0.5^\circ \times 0.5^\circ$ spatial resolution, covering the period from 1957 to 2001.

Within the ATREUS network, the Baixa neighbourhood in Lisbon was selected for simulations (Oxizidis et al. 2007). MM5 domains over Lisbon were defined as shown in Fig. 2. Four nested domains were identified with increasing spatial resolution from 27 km (domain 1) to 1 km (domain 4). The intermediate domains 2 and 3 have resolutions of 20 km and 4 km, respectively. The Baixa area was the subject of previous CFD pollutant dispersion study by Borrego et al. (2003).

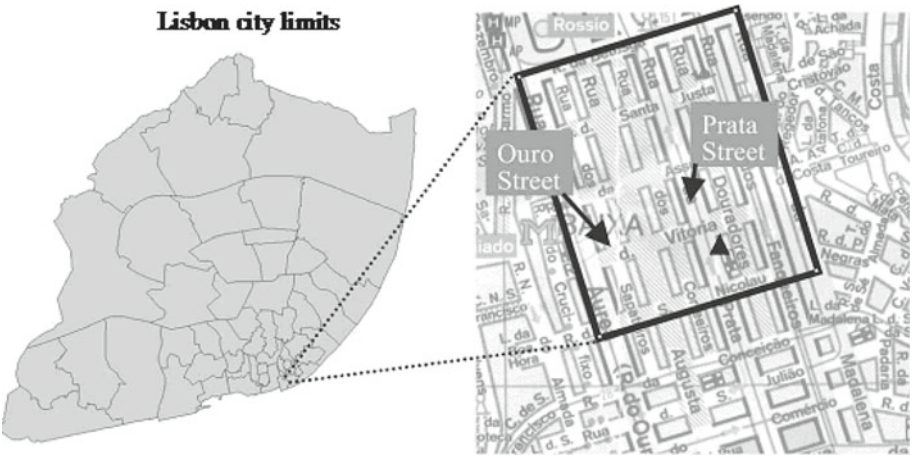

Fig. 3 Area of Lisbon centered on Baixa. The *bold line* outlines the limits of the Baixa area (adapted from Borrego et al. 2003)

Baixa is located in the southern part of Lisbon, between the river Tagus and the Atlantic Ocean. The area is characterised by homogeneously distributed buildings, consisting of well-aligned arrays of blocks with uniform height $H = 15\,\mathrm{m}$. The Baixa area is aligned with a frame of reference rotated clockwise by 344° with respect to north (Fig. 3). The planar area A_p of Baixa is $450 \times 450\,\mathrm{m}^2$, which falls in the neighbourhood scale defined in Sect. 2. The canopy planar area density λ_p (the ratio of the total roof area to A_p), is equal to 0.33. The frontal area density λ_f (the ratio of the frontal area of the building affected by the wind to A_p) is more important to the drag because it represents the surface facing the airflow. Consequently, λ_f depends on the incoming wind direction θ. Eight wind directions were analysed, of equal intervals of 45° (with respect to the Baixa orientation). $\lambda_f(\theta)$ was calculated using the methodology discussed by Ratti et al. (2002), based on digital elevation model (DEM) data. The zero-plane displacement height, d and aerodynamic roughness length, z_0 (which also depends on θ) were calculated according to Macdonald et al. (1998):

$$d = \left(1.0 + 4.2^{-\lambda_p}(\lambda_p - 1.0)\right) H, \tag{2}$$

$$z_0(\theta) = \left(1.0 - \frac{d}{H}\right) \exp\left[-\left(\frac{C_D}{\kappa^2}\left(1.0 - \frac{d}{H}\right)\lambda_f(\theta)\right)^{-0.5}\right], \tag{3}$$

in which $C_D = 1.2$ is the drag coefficient. Parameterisations (2) and (3) were obtained by Macdonald et al. (1998) for array of cubes and have the advantage of being based on readily available input data. The numerical coefficient 4.2 in Eq. 2 has been obtained as an average of the values given by Macdonald et al. (1998). Its variation, however, has little influence on the results and it is not central to the scope of our study.

Geometrical features of the Baixa neighbourhood are summarised in Table 1. Results showed that for the investigated λ_f and λ_p, the roughness length and the displacement height are close to the rule-of-thumb values of $0.1H$ and $0.66H$ respectively, suggested by Grimmond and Oke (1999), as well as within the range of variability suggested by Britter and Hanna (2003).

For the purposes of ATREUS, 9 July 2000 was chosen as representative of the most frequent circulation weather type in Lisbon, to reproduce hourly vertical profiles of wind speed

Table 1 Geometrical features and morphological parameters of the Baixa area

Planar area (m^2)	$\lambda_f(\theta)$	λ_p	H (m)	d (m)	z_0 (m)
450 × 450	0.07–0.36	0.33	15.0	8.8	$0.07H$–$0.15H$

and temperature over the Baixa area (Oxizidis et al. 2007). The selected day was characterised by wind speeds in the range 5.0 to 13.0 m s^{-1} at a height of $3H$, and prevailing wind direction from the south. Pressure, temperature, humidity, turbulent kinetic energy and vertical profiles of wind speed and direction, were generated from MM5 simulations over Baixa for the selected day. MM5 simulations provided vertical profiles of the meteorological variables starting from $z_t \approx 10$ m, up to approximately 1200 m ($u(z < z_t) = 0$ in MM5). Shear stress, latent and sensible heat fluxes at the ground ($z = 0$ m) were also provided by MM5.

3.2 The Urban Model

A simple urban model was developed to derive vertical profiles of mean wind speed and temperature within the urban canopy, from $z = 3H$ down to the ground.

The aim of the urban model is to produce more accurate solutions for the wind profiles within the urban canopy layer, and to offer a simple and cost-effective parameterisation for the spatial distribution of the temperature within the urban canopy layer. The urban model developed in our study uses the mass exchange formulation based on the exchange velocity u_E. The transfer of mass is the main process responsible for the scalar exchange of heat, moisture, and other scalar quantities such as pollutants, between the urban canopy layer and the urban boundary layer above. The exchange velocity formulation u_E proposed by Bentham and Britter (2003) was applied to obtain spatially-averaged temperature profiles within the urban canopy layer:

$$u_E = \frac{u_\star^2}{u_{3H} - U_C} \tag{4}$$

where u_{3H} is the wind speed at the reference height z_{3H}, $u_\star$ is the friction velocity and U_C is the in-canopy wind speed. The velocity scale u_E is related to the momentum flux at the top of the urban canopy layer, and represents an exchange between two flows, that of the urban canopy layer (identified with U_C) and that of the inertial sublayer (identified with u_{3H}). Various formulations for U_C are discussed in Sect. 4.2.

The model adopted here for the calculation of the spatially-averaged mean wind profiles is that developed and validated by Di Sabatino et al. (2008) for the case of uniform (cube-type of roughness) and non-uniform (buildings in urban areas) spatial distributions of roughness elements. It is based on the momentum balance between the urban canopy layer and the atmosphere above. This is expressed in terms of the drag force exerted by the various land-use elements on the airflow as:

$$\frac{d}{dz}\left(l(z,L)\frac{du(z)}{dz}\right)^2 = \frac{1}{A_p}\left(\sum_{i=1}^{n_{land-use}} \frac{C_{D,i}\lambda_{f,i}}{2H_i} A_{p,i}\right) u(z)^2 \tag{5}$$

in which $u(z)$ is the spatially-averaged wind profile. Parameters $C_{D,i}$ (the drag coefficient), H_i (the averaged height of the roughness elements), and $\lambda_{f,i}$ (the frontal area density affected by the wind) are relative to the associated land-use category, each weighted with the corresponding portion of land-use area $A_{p,i}$. For example, if the area being analysed is composed of 70% buildings and 30% trees, the weighting factor would be 0.7 and 0.3 for buildings and

trees respectively. $\sum_i A_{p,i} = A_p$ is the total planar area of the neighbourhood. When Eq. 5 is applied to urban areas, only land-use categories with roughness element heights comparable to that of the buildings contribute to the drag on the mean flow. That is, only trees and other man-made structures should be incorporated. For the Baixa area analysed here, $A_{p,i} \neq 0$ only for buildings. Therefore, Eq. 5 for Baixa simplifies with H, λ_f, and C_D the mean height, the frontal area density, and the drag coefficient of buildings, respectively.

Atmospheric stability effects in terms of the Obukhov length scale L are included in the expression for the mixing length l to yield:

$$l(z, L) = \begin{cases} H - d & z \leq H \\ \kappa z \Psi(z/L) & z > H \end{cases}, \tag{6}$$

where $\Psi(z/L)$ reads (Businger et al. 1971; Dyer 1974):

$$\Psi(z/L) = \begin{cases} 1 + 4.7z/L & z/L \leq 0, \\ (1 - 15z/L)^{-0.25} & z/L > 0. \end{cases} \tag{7}$$

Using MM5 data from the nearest grid point to Baixa and parameters in Table 1, Eq. 5 was applied to calculate the spatial-averaged wind profiles over the Baixa area. Boundary conditions, in terms of u, du/dz, and wind direction were specified at z_{3H}. It is worth remarking that one of the main novelties introduced by Eq. 5 is that the boundary condition is not prescribed in terms of the no-slip condition $u(z = 0) = 0$ (e.g. Cionco 1965; Coceal and Belcher 2004). As observed by Di Sabatino et al. (2008), such a condition is inappropriate in a model that does not resolve the building geometry or treat the roughness of the various constituent surfaces (ground, building walls, etc.) By contrast, by specifying u and du/dz at the top of the investigated area, the shape of the mean flow profile is solely controlled by the drag through λ_f.

Equation (5) assumes that the wind is representative of the investigated neighbourhood area. Consequently, the mean wind speed is equivalent to the spatially-averaged wind speed over the area available for the flow. The roughness elements within the urban canopy layer exert a drag force on the local airflow, whose effects are represented as a body force. This approach avoids the unnecessary detail and the large computational costs to resolve the flow around individual buildings. Moreover, the simple model based on Eq. 5 has the advantage of being easily extended to an operational context, as it requires few input parameters, namely H and the morphological parameter λ_f. The use of Eq. 5 may require that the investigated area is statistically homogeneous. This can be achieved by fulfilling some morphological conditions, e.g. that the standard deviation of the building height σ_H in the investigated area is small. Such model requirements are extensively discussed by Di Sabatino et al. (2008). For the case analysed herein, the selected area does not differ substantially from a regular array of cubes, being characterised by well aligned buildings of the same height, for which $\sigma_H \approx 0.0$. For this particular scenario the model based on Eq. 5 was successfully validated by Di Sabatino et al. (2008).

The exchange velocity u_E (Eq. 4) has been applied for calculating the sensible heat flux density Q_H (W m^{-2}) between the urban canopy layer and the inertial sublayer, which can be approximated as (Solazzo and Britter 2007):

$$Q_H = \rho C_p u_E (T_{can} - T_{3H}) \tag{8}$$

where ρ (kg m^{-3}) is the density of the air, C_p (J K^{-1} kg^{-1}) is the specific heat capacity at constant pressure of the air, and T_{3H} (K) is the air temperature at the reference height z_{3H}. u_E (m s^{-1}) is the exchange velocity calculated as in Eq. 4, using $u_\star$ from MM5 calculations.

According to Solazzo and Britter (2007), the temperature distribution at street scale and within the urban canopy layer, T_{can}, is considered as well mixed, and thus spatially homogeneous (in a spatially-averaged sense). In this study the spatially-averaged temperature of the whole urban canopy layer, T_{can}, has been evaluated using Eq. 8 and assuming that the heat flux was known:

$$T_{can} = T_{3H} + \frac{Q_H}{\rho C_p u_E} \tag{9}$$

In Eq. 9, Q_H and T_{3H} were provided by the MM5 simulations. To each land-use category, MM5 associates the thermal properties of albedo, heat capacity, and heat conductivity. Based on these features and meteorological conditions, the heat flux density is evaluated. Detail of these calculations are given in Oxizidis et al. (2007).

The set of equations (4), (5), and (9) forms the core of the urban model proposed in our study, which has been tested for the selected day, 9 July 2000, over the Baixa neighbourhood.

4 Results and Discussion

4.1 Friction Velocity

Friction velocity values were estimated from Eq. 1, with $u = u_{3H}$ and $z = 3H$:

$$\frac{u_\star}{u_{3H}} = \frac{\kappa}{\ln(z_{3H} - d) - \ln(z_0(\theta))} \tag{10}$$

Results shown in Fig. 4 highlight some important aspects. Hourly variations of $u_\star/u_{3H}$ derived from Eq. 10 are determined by the wind direction. Oscillations of the MM5 data for the normalised $u_\star$ are due to the hourly variation of the wind direction and of the stability, whereas the values of d and $z_0(\theta)$ in Eq. 10 were calculated using Eqs. 2 and 3 for intervals of 45° (see Sect. 3.1). Within MM5, z_0 and d do not depend "directly" on wind direction, in the sense that there is not an explicit relationship expressing them as a function of wind direction. There is, though, an "indirect" effect of the wind direction on the mean flow, which is due to the different z_0 values associated with each land-use category surrounding the Baixa area. Because the oncoming flow approaching Baixa is affected by the underlying roughness, depending on wind direction, departure from equilibrium is expected, which translates into a $u_\star/u_{3H}$ variation.

In our approach, the normalised friction velocity from Eq. 10 is calculated by assuming that the flow is in equilibrium with the Baixa area, and in this respect is a function of the local morphology. The value calculated by MM5 provides an independent calculation of friction velocity. In this latter case it depends on the upstream fetch and atmospheric stability. Figure 4 shows that the two approaches give comparable values of the friction velocity. Some features of the inertial sublayer are discussed in more detail in Sect. 4.3. To explain the similar trend (i.e. the hourly variation) of the two sets of data in Fig. 4, however, the data available do not allow general conclusions to be drawn at this stage, and further investigations are required.

Results in Fig. 4 show that $u_\star$ is in the range of 10 to 14% of the reference wind speed, u_{3H}. These values agree well with the local friction velocity at $z = 3H$ (based on an average over a large number of full-scale observations) reported by Roth (2000), who found $u_\star/u_{3H} \approx 0.11$.

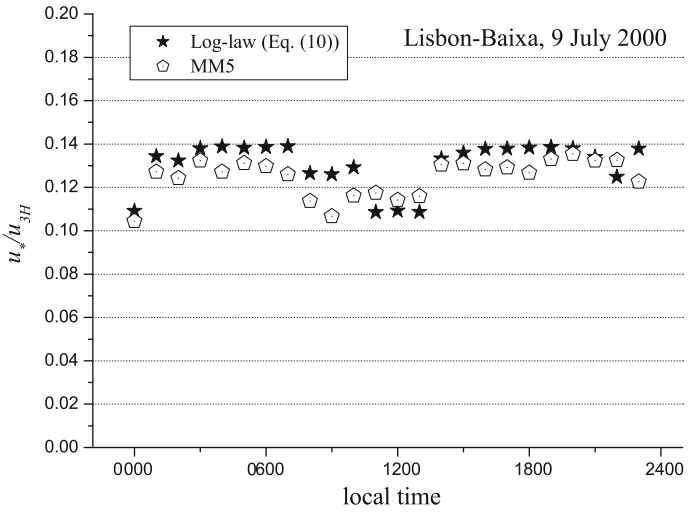

Fig. 4 Normalised friction velocity

4.2 In-Canopy Velocity

The in-canopy wind speed U_C is a scale for the estimation of the spatially-averaged wind speed within the urban canopy layer. U_C can be used in operational dispersion models to quantify the advective transport within the urban canopy. In our study, U_C was calculated by comparing four different formulations, from which one was then selected to proceed with the investigation. The formulations were derived from the following:

– U_C from $u(z)$ (Eq. 5), defined as the spatially-averaged wind speed within the canopy:

$$U_C = \frac{1}{H}\int_0^H u(z)dz. \tag{11}$$

– U_C from the formulation proposed by Bentham and Britter (2003):

$$U_C = u_\star\sqrt{\frac{2.0}{\lambda_f}}, \tag{12}$$

where $u_\star$ was obtained from MM5 simulations.

– U_C from a modified version of Eq. 12, which was formulated for low λ_p values. Equation (12) has been extended to any value of λ_p, with the requirement $lim_{\lambda_p\to 1}U_C(\lambda_p) = 0$. Incorporating these modifications yields:

$$U_C = u_\star\sqrt{\frac{2.0}{\lambda_f}}(1.0-\lambda_p). \tag{13}$$

– U_C from the analytical formulation proposed by Macdonald (2000), using $u(z) = u_H\exp(-a(1.0-z/H))$, which integrated over $[0, H]$ and divided by H gives:

$$U_C = \frac{u_H}{a}(1.0-e^{-a}) \tag{14}$$

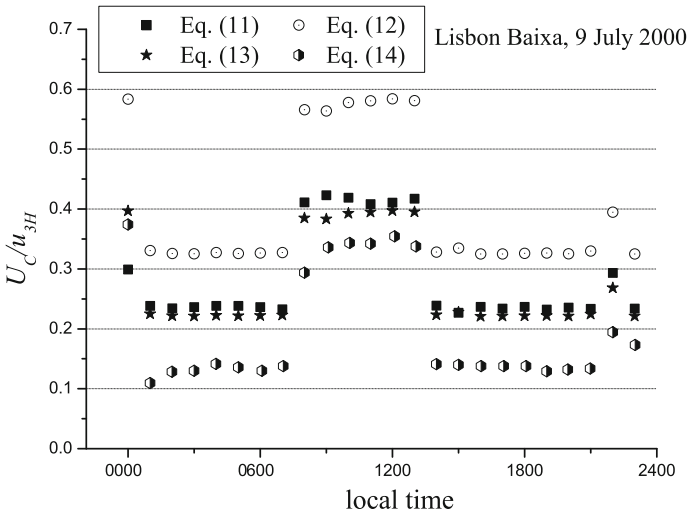

Fig. 5 Comparison between several formulations of U_C for the Baixa area

where a is the attenuation coefficient ($a = 9.6\lambda_f$, Macdonald 2000) and u_H is the horizontal wind speed at $z = H$ obtained from Eq. 5.

Results in Fig. 5 show that Eqs. 11 and 13 predict very similar values, with U_C in the range 20 to 40% of u_{3H}, depending on the wind direction. Results from Eq. 12 are about 30% larger, whereas results from Eq. 14 are lower than those of the previous two formulations. Equation (14) depends on a larger number of additional parameters, such as the attenuation coefficient and the roof top wind speed, which are usually difficult to measure. For consistency with the downscaling approach based on Eq. 5, U_C derived from Eq. 11 has been adopted in our study. It is worth observing that λ_p is introduced in Eq. 11 through the mixing length (Eq. 6), which is $l = H - d$ for $z \leq H$. Since $lim_{\lambda_p \to 1} d = H$, it follows $lim_{\lambda_p \to 1} l = 0$, and thus $U_C(\lambda_p = 1) = 0$.

Results in Fig. 5 also show a sharp increase between 0800 and 1400 local time (LT), which corresponds to a trend similar to that already observed for the normalised $u_\star$ shown in Fig. 4. This clearly shows the dependence of λ_f on wind direction. All formulations for U_C compared in Fig. 5 depend on λ_f and are derived from Eq. 5, which explains the trend in the figure. The only exception are Eqs. 12 and 13 that use $u_\star$ from MM5 and depend on λ_f explicitely.

4.3 Spatially-Averaged Mean Wind-Speed Profiles

Two examples of the solution of Eq. 5 are displayed in Fig. 6, which resemble the schematic profiles shown in Fig. 1. The two cases refer to two different hours, and were selected for the value of λ_f, which is low in the first case ($\lambda_f = 0.07$, Fig. 6a) and high in the second case ($\lambda_f = 0.36$, Fig. 6b). Both, the spatially-averaged mean wind speed $u(z)$ and the wind-speed profile computed by MM5 are normalised with the reference wind speed, u_{3H}. For comparison, Eq. 5 was also solved above z_{3H}, by using u_{3H} as boundary condition at the bottom. In this case the right-hand side of Eq. 5 is zero, and the derivative $\mathrm{d}u_{3H}/\mathrm{d}z$ was also provided as a boundary condition. From the two graphs in Fig. 6, MM5 and Eq. 5 predict the same wind-speed profile within the inertial sublayer, above z_{3H}. Below z_{3H}, Eq. 5 predicts lower values. In fact, the mean wind speed here is strongly influenced by the drag exerted

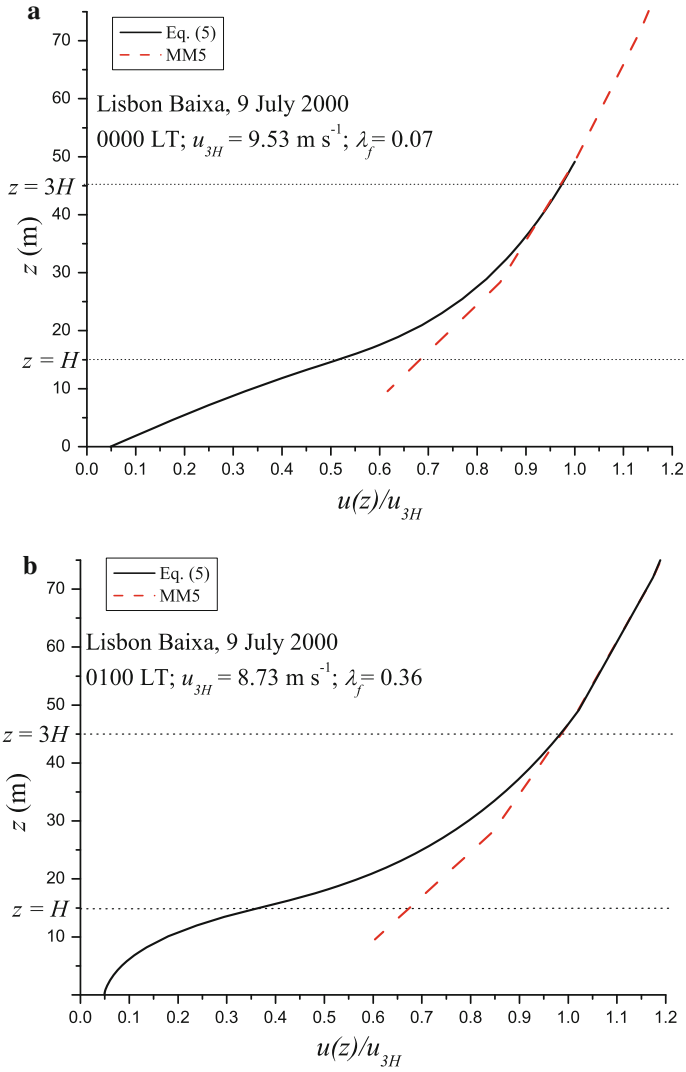

Fig. 6 Spatially-averaged mean wind speed profile for **a** 0000 LT, and **b** 0100 LT of the selected day 9 July 2000 for the Baixa neighbourhood in Lisbon. Outputs from Eq. 5 and MM5 are compared, for different λ_f

by the buildings below $z = H$, which is felt throughout the roughness sublayer. Wind-speed profiles predicted by MM5 clearly show that the model does not represent the effect of the underlying buildings on the airflow.

Effects of the frontal area density λ_f are also evident by comparing the two curves in Fig. 6. For $\lambda_f = 0.36$, the inflexion of the mean wind speed for $z \leq H$ indicates a wind-speed reduction. For $\lambda_f = 0.06$, the spatially-averaged wind-speed profile is well approximated by a straight line (Fig. 6a), indicating the poor resistance of the buildings on the airflow. A linear trend of the mean wind-speed profile for $z \leq H$ has been also found in the computational study by Martilli and Santiago (2007) for an array of cubes with $\lambda_f = 0.25$, and in the

water flume experiment by Macdonald (2000), for $\lambda_f = 0.16$. Thus, it may be argued that a trend does exist for $\lambda_f \leq 0.25$ (at least), for which the spatially-averaged wind speed profile within the urban canopy layer obeys a linear law. For $\lambda_f = 0.44$, experimental data by Macdonald (2000), and the theoretical study by Di Sabatino et al. (2008), showed that an exponential-based function provides a better accuracy than a straight line as far as replicating the mean wind speed within the urban canopy layer. Similar conclusions were also drawn with the simple model developed by Cionco (1965) for the spatially-averaged mean wind speed within a vegetative canopy. In the case of Fig. 6b, it can also be observed that for $\lambda_f = 0.36$ a simple straight line would not provide a good estimation of $u(z)$ for $z < H$.

It is also worth to notice that different wind-speed profiles below $z = H$ imply different U_C values. In fact, results from Eqs. 11 and 13 in Fig. 5 show that the spatially-averaged U_C is about 20% larger at 0000 LT (corresponding to $\lambda_f = 0.06$), than at 0100 LT (corresponding to $\lambda_f = 0.36$).

Results based on Eq. 5 give more detailed wind-speed profiles. Moreover, the simple model based on Eq. 5 is fast to run because it does not require large computational costs. Thus, it could be implemented within MM5 (or other similar models) to give an initial estimation of the urban effect on the airflow within the urban canopy layer, which would allow for the improvement of the simple parameterisation given by Eq. 1 within the roughness sublayer.

4.4 Urban Heat Island Effect

Spatially-averaged temperature profiles remove the sensitivity associated with individual measurement points within the urban area. Kanda et al. (2005) argued that temperature profiles within the urban canopy layer are strongly related to the location where measurements are collected, due to the diversity of surface materials and geometries. One of the advantages of using T_{can} from Eq. 9 is that it provides an initial estimation of the canopy temperature as a whole, regardless of the specific location within the urban canopy layer.

Results for T_{can} and T_{3H} are shown in Fig. 7, where the crosses indicate the normalised exchange velocity u_E, which is controlled by the friction velocity in Eq. 4. It can be observed that u_E is within the range 2.0 to 2.5% of u_{3H}. Such a result is in good agreement with other CFD-based studies, where u_E was estimated from the transfer of scalar tracers, such as heat (Solazzo and Britter 2007), and mass release (Hamlyn et al. 2007).

From Fig. 7 it can be observed that the maximum difference between T_{can} and T_{3H} corresponds to a minimum of u_E, as expected from Eq. 9. The maximum difference for the investigated day was detected at 1200 LT, with a temperature difference of about 3 K. Similarly, between 1000 LT and 1300 LT the temperature difference was approximately 2.5 K. During the time periods 0000 LT to 0700 LT, and 2000 LT to 2300 LT, the simple model based on Eqs. 4 and 9 predicted a smaller difference between the temperature within the urban canopy layer and that at z_{3H} (of approximately 1 K).

The canopy temperature T_{can} is also compared with T_{out}, which was measured at a height of 2 m above the ground at the Cacem meteorological station, located in the outskirts of Lisbon. The determination of the air temperature in the urban canopy allows the calculation of ΔT_{UHI}, defined as:

$$\Delta T_{UHI} = T_{can} - T_{out}, \tag{15}$$

which represents the difference between the air temperature in the urban canopy layer and the air temperature recorded at a close meteorological station, in the surrounding rural part of the city. Calculation of ΔT_{UHI} provides an estimation of the UHI in Lisbon during the selected day (Oke 1992). Peak differences between T_{can} and T_{out} of about 5.5 K were found

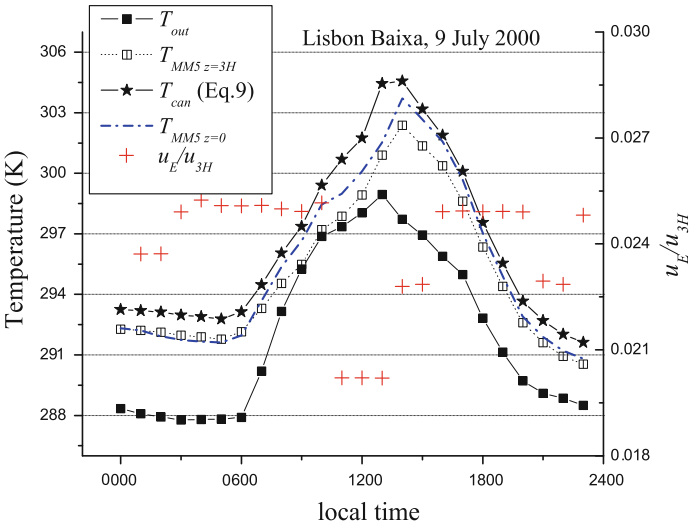

Fig. 7 Temperatures (*left hand side axis*) and normalised exchange velocity (*right hand side axis*) time series. T_{out}: temperature measured at the Cacem meteorological station; $T_{MM5z=3H}$: reference temperature provided by MM5; $T_{MM5z=0}$: temperature at the ground predicted by MM5; T_{can}: temperature of the urban canopy layer from Eq. 9

between 1300 LT and 1600 LT. A large UHI effect is also evident during the night, between 0000 LT and 0700 LT, with $\Delta T_{UHI} \approx 4.5$ K. Between 0800 LT and 1000 LT the UHI is at the minimum, with $\Delta T_{UHI} \approx 1.5$ K. Finally, ΔT_{UHI} is almost constant after 1700 LT, equal to approximately 3 K. Alcoforado and Andrade (2006) reported a mean nocturnal UHI in Lisbon of approximately 2.5 K, with a peak of 4 K, based on field measurements. Results obtained in our study are not far from those findings, although based on the calculation of a single day. It is worth pointing out that unbiased models are assumed in estimating the UHI in Eq. 15, given that "modelled" urban temperature and "measured" rural temperature are compared.

In Fig. 7 the ground level temperature predicted by MM5, $T_{MM5z=0}$ is also reported. This temperature is estimated by the model by considering the thermal properties of the Baixa area and it does not include any "canopy effect". Therefore, the difference between $T_{MM5z=0}$ and T_{can} are due to the urban model developed in our study. $T_{MM5z=0}$ and T_{3H} exhibit a similar trend during nighttime hours. Between 0900 LT and 1400 LT the difference is more pronounced due to the larger heat flux density Q_H. During this time lag the difference between T_{can} and $T_{MM5z=0}$ is more evident, with peak differences of approximately 2 K at 1200 LT, but much smaller than the values predicted by means of Eq. 15.

Finally, it should be noticed that for the case of sensible heat fluxes, field data or more detailed models could be used to estimate Q_H, (for example, see the radiative model proposed by Lee and Park (2008) and by Kusuka and Kimura (2004)). Nevertheless, this would not change the simplicity of the methodology based on Eq. 9.

5 Conclusions and Future Work

Accurate modelling of the flow field and temperature patterns inside the roughness sublayer is one of the key aspects for assessing the energy consumption of buildings as well as for

investigating pollutant dispersion at neighbourhood scales and below. The assumption of a simple roughness parameterisation may result in poorly detailed results at such scales. On the other hand, very detailed formulations accounting for the effects of the city area within NWP models may require large computational resources and numerous input data. Therefore, a simple urban parameterisation has been developed to be coupled with mesoscale models, such as MM5, to output meteorological profiles within the urban canopy layer. Furthermore, the model proposed is simple to run and requires few input parameters, requiring no additional computational costs.

The urban model is based on the spatially-averaged mean profiles of wind speed and temperature. A drag-force approach is used to represent the dynamic and turbulent effects of the buildings on the flow, and a mass transfer parameterisation is used to take into account urban thermal effects on the flow. The urban model was used for a real application for the city of Lisbon (Portugal) where the Baixa neighbourhood was selected for analyses. Hourly variations of several meteorological variables over 24 hours were analysed. Three velocity scales were quantified, each of direct usefulness for dealing with the flow, the dispersion, and the exchange processes in urban areas. The following results were obtained:

- The friction velocity $u_\star$ was found to be between 10 and 14% of the reference wind speed u_{3H}.
- The spatially-averaged in-canopy wind speed U_C was found to be highly sensitive to the formulation applied for its calculation. Results obtained in our study suggest that $U_C \approx 0.3u_{3H}$ offers a valid estimation, calculated as an integral velocity averaged over the height of the canopy layer.
- The exchange velocity u_E was found to vary within the range 2.0 to 2.5% of u_{3H}. We note that u_E is the main parameter controlling the transfer of mass between the urban canopy layer and the atmospheric layer above.
- The variations with time of the aforementioned variables indicate that the flow field and the turbulence within the urban canopy layer are mainly controlled by the wind direction, which, in our model is accounted for by λ_f and z_0.
- Results derived from the mass exchange analyses showed a canopy effect (differential temperature between the canopy and the reference height of $3H$ above the canopy), with a maximum of 3 K between 1200 and 1400 local time, and negligible during the nighttime hours. Moreover, a urban heat island effect (differential temperature between the canopy and a location outside the urban area) of an average of 3 K was calculated for the selected day.

The results presented herein provide the basis for future research. The limitations of the developed model will be the starting point of further investigations. For example, it is important to test the model sensitivity to other formulations of the parameters d, z_0, C_D, and l. Analyses on the urban heat island and $u_\star$ should also be extended to other days and possibly to other urban areas for which more accurate information on heat flux density and shear stress are available. The model for momentum balance between the urban canopy and the inertial sublayer assumes that all momentum sources derive from the pressure and viscous drag forces from the vertical building surfaces. Considering additional sources, such as from horizontal building surfaces (e.g. Dupont et al. 2004), can also contribute to improve our model.

The model developed in our study can be extended to any scalar whose transfer is driven by the mass exchange at the urban canopy layer interface. Therefore, the exchange of latent heat flux, pollutants, heat, and others, could be analysed based on the hypothesis that any scalar is homogeneously mixed within the urban canopy layer.

Acknowledgments This study was partially conducted within the Research Training Network ATREUS (Contract No. HPRN-CT-2002-00207), funded by the European Commission, Training and Mobility of Researchers Programme. The authors wish to thanks all the participants in the project. Rex Britter was funded in part by the Singapore National Research Foundation (NRF) through the Singapore-MIT Alliance for Research and Technology (SMART) Center for Environmental Sensing and Modeling (CENSAM).

References

Alcoforado M-J, Andrade H (2006) Nocturnal urban heat island in Lisbon (Portugal): main features and modelling attempts. Theor Appl Climatol 84:151–159

Bentham T, Britter RE (2003) Spatially averaged flow within obstacle arrays. Atmos Environ 37: 2037–2043

Best MJ (2005) Representing urban areas within operational numerical weather prediction models. Boundary-Layer Meteorol 114:91–109

Borrego C, Tchepel O, Costa AM, Amorim JH, Miranda AL (2003) Emission and dispersion modelling of Lisbon air quality at local scale. Atmos Environ 37:5197–5205

Britter RE, Hanna SR (2003) Flow and dispersion in urban areas. Annu Rev Fluid Mech 35:469–496

Businger JA, Wyngaard JC, Izumi Y, Bradley EF (1971) Flux-profile relationships in the atmospheric surface layer. J Atmos Sci 28:181–189

Cheng H, Castro IP (2002) Near wall flow over urban-like roughness. Boundary-Layer Meteorol 104: 229–259

Cionco R (1965) A mathematical model for air flow in a vegetative canopy. J Appl Meteorol 4:517–522

Coceal O, Belcher SE (2004) A canopy model of mean winds through urban areas. Q J Roy Meteorol Soc 130:1349–1372

Di Sabatino S, Solazzo E, Paradisi P, Britter R (2008) A simple model for spatially-averaged wind profiles within and above an urban canopy. Boundary-Layer Meteorol 127:131–151

Dudhia J, Bresch JF (2002) A global version of the PSU-NCAR mesoscale model. Mon Weather Rev 130:2989–3007

Dupont S, Otte TL, Ching JKS (2004) Simulation of meteorological fields within and above urban and rural canopies with a mesoscale model (MM5). Boundary Layer Meteorol 113:111–158

Dyer AJ (1974) A review of flux-profile relationships. Boundary-Layer Meteorol 7:363–372

Grimmond S, Oke T (1999) Aerodynamic properties of urban areas derived form analysis of surface form. J Appl Meteorol 38:1261–1292

Hamlyn D, Hilderman T, Britter RE (2007) A simple network approach to modelling dispersion among large groups of obstacles. Atmos Environ 41:5848–5862

Kanda M, Moriwaki R, Kimoto Y (2005) Temperature profiles within and above an urban canopy. Boundary-Layer Meteorol 115:499–506

Kastner-Klein P, Rotach MW (2004) Mean flow and turbulence characteristics in an urban roughness sublayer. Boundary-Layer Meteorol 111:55–84

Kusaka H, Kimura F (2004) Coupling a single-layer urban canopy model with a simple atmospheric model: impact on urban heat island simulation for an idealized case. J Meteorol Soc Jpn 82:67–80

Lee S-H, Park S-U (2008) A vegetated urban canopy model for meteorological and environmental modelling. Boundary-Layer Meteorol 126:73–102

Macdonald RW (2000) Modelling the mean velocity profile in the urban canopy layer. Boundary-Layer Meteorol 97:25–45

Macdonald R, Griffiths RF, Hall DJ (1998) A comparison of results from scaled field and wind tunnel modelling of dispersion in arrays of obstacles. Atmos Environ 32:3845–3862

Martilli A (2007) Current research and future challenges in urban mesoscale modelling. Int J Climatol 27:1909–1918

Martilli A, Santiago JL (2007) CFD simulation of airflow over a regular array of cubes. Part II: analysis of spatial average properties. Boundary-Layer Meteorol 122:635–654

Martilli A, Cappier A, Rotach MW (2002) An urban surface exchange parameterisation for mesoscale models. Boundary-Layer Meteorol 104:261–304

Oke TR (1992) Boundary layer climates. Methuen, London

Oxizidis S, Dudek A, Papadopoulos AM (2007) A computational method to assess the impact of urban climate on buildings using modelled climatic data. Energy Build 40:215–223

Papadopoulos AM, Moussiopoulos N (2004) Towards an holistic approach for the urban environment and its impact on energy utilization in buildings: the ATREUS project. J Environ Monit 6:841–848
Ratti C, Di Sabatino S, Britter RE, Brown M, Caton F, Burian S (2002) Analysis of 3-D urban database with respect to pollution dispersion for a number of European and American cities. Water Air Soil Pollut 2:459–469
Roth M (2000) Review of atmospheric turbulence over cities. Q J Roy Meteorol Soc 126:941–990
Solazzo E, Britter RE (2007) Transfer processes in a simulated urban street canyon. Boundary-Layer Meteorol 124:43–60